Journal of Organometallic Chemistry, 394 (1990) 777–794
Elsevier Sequoia S.A., Lausanne
JOM 21199

Flexible coordination of indenyl ligands in sandwich complexes of transition metals. Molecular structures of $[(\eta\text{-}C_9R_7)_2M]$ (M = Fe, R = H, Me; M = Co, Ni, R = H): direct measurement of the degree of slip-fold distortion as a function of *d*-electron count *

Steve A. Westcott, Ashok K. Kakkar, Graham Stringer, Nicholas J. Taylor * and Todd B. Marder *

Department of Chemistry, University of Waterloo, Waterloo, Ontario N2L 3G1 (Canada)

(Received February 13th, 1990)

Abstract

The crystal and molecular structures of $[(\eta\text{-}C_9H_7)_2M]$ (M = Fe, **1**; Co, **2**; Ni, **3**) and $[(\eta\text{-}C_9Me_7)_2Fe]$, **4**, are reported, along with a discussion of the correlation between hapticity and the ^{13}C chemical shift of the indenyl ring-junction carbons (C(3a), C(7a)). Single crystals of both **1** and **2** undergo non-destructive and reversible phase changes upon cooling below ca. 240–245 K. The room-temperature structures are disordered; however, the low temperature ones (150 K) are essentially ordered. Crystals of **3** do not display this behavior on cooling to 150 K, and residual anisotropy in certain carbon atoms is ascribed to a minor twinning problem. Crystals of **4** were only examined at ambient temperature, where an ordered structure was obtained.

In contrast to the analogous Cp_2M series ($Cp = \eta^5\text{-}C_5H_5$; M = Fe, Co, Ni), which display a gradual symmetric increase in M–C distances in the order Fe < Co < Ni, the distortions in the indenyl series are of a fundamentally different nature. Thus, there is a gradual increase in the degree of slip-fold distortion from η^5- toward η^3-coordination which involves (a) slippage of the metal away from C(3a),C(7a), and (b) folding of the ring system (particularly at C(1),C(3)), in the order Fe < Co < Ni.

The slip values (Δ = avg d(M–C(3a),C(7a)) – avg d(M–C(1),C(3)) are 0.043(4), 0.124(4), 0.418(6), and 0.030(4) Å for **1**–**4**, respectively. For a "true η^5-"complex, Δ should be ca. 0 Å, whereas values of ca. 0.69–0.79 Å have been reported for "true η^3-"indenyl complexes such as $[(\eta^3\text{-}C_9H_7)Ir(PMe_2Ph)_3]$. Therefore, complexes **1** and **4** are clearly η^5, as predicted on the basis of the 18-electron rule, whereas **2** and **3**

* Dedicated to Professor Gordon Stone on the occasion of his 65th birthday.

display increasing degrees of distortion in both rings to avoid 19- and 20-electron counts, respectively. The two indenyl rings in **3** are half-way between η^5- and η^3-coordination modes.

Crystal data for **1** at 295 K are: monoclinic, $P2_1/n$, a 8.030(2), b 7.806(2), c 10.779(2) Å, β 107.39(1)°, V 648.9(2) Å^3, $Z = 2$, structure not refined; at 150 K: monoclinic, Cc, a 16.021(4), b 15.510(5), c 11.187(3) Å, β 115.53(2)°, V 2509(1) Å^3, $Z = 8$, $R = 0.0306$, $R_w = 0.0332$. For **2** at 295 K: monoclinic, $P2_1/n$, a 8.027(2), b 7.838(2), c 10.936(3) Å, β 107.57(2)°, V 655.9(2) Å^3, $Z = 2$, structure not refined; at 150 K: monoclinic, $P2_1/c$, a 11.258(3), b 7.824(3), c 15.256(6) Å, β 108.07(2)°, V 1277.7(7) Å^3, $Z = 4$, $R = 0.0397$, $R_w = 0.0447$. For **3**, at 150 K: monoclinic, $P2_1/n$, a 6.063(1), b 20.056(3), c 10.703(2) Å, β 94.27(1)°, V 1297.9(3) Å^3, $Z = 4$, $R = 0.0413$, $R_w = 0.0493$. For **4**, at 295 K: orthorhombic, $Pbcn$, a 14.211(2), b 9.284(2), c 19.289(4) Å, V 2544.8(8) Å^3, $Z = 4$, $R = 0.0410$, $R_w = 0.0421$.

Introduction

It is well known that [(η^5-indenyl)ML_n] complexes display enhanced reactivity in both S_N1 [1,2] and S_N2 [1–5] substitution reactions, compared with their cyclopentadienyl analogues. In addition, enhanced catalytic activity has been demonstrated for [(η^5-indenyl)ML_2] complexes (M = Co, Rh; L = alkene) in intermolecular hydroacylation reactions [6], cyclotrimerization of alkynes to benzenes [7], and cyclocotrimerization of alkynes and nitriles to pyridines [8]. Recent kinetic studies [2,4] and the isolation and structural characterization of three stable [(η^3-C_9H_7)ML_n] complexes, [(η^3-C_9H_7)Ir(PMe_2Ph)$_3$], **5** [9], [(η^3-C_9H_7)Fe(CO)$_3$]$^-$, **6** [10], and [(η^3-C_9H_7)(η^5-C_9H_7)W(CO)$_2$], **7** [11], indicate the relative ease of slippage of the indenyl ring from η^5- to η^3-coordination during S_N2 substitution reactions at 18-electron metal centers. The decreased hapticity accommodates the extra electron pair of the incoming nucleophile, alleviating an unfavorable 20-electron count at the metal center. Dissociation of the leaving ligand results in a return to the η^5-coordination mode of the indenyl moiety.

The relative ease of ring slippage for indenyl vs. cyclopentadienyl ligands has generally been attributed [1–4] to the rehybridization of the indenyl π-system, which involves an increase in the aromatic character of the benzene ring. This results in a disruption of the aromatic character in the five-membered ring and thus, would be a higher energy process for cyclopentadienyl ligands (Scheme 1).

During the course of our continuing investigations of the solid-state structures, solution dynamics, reactivity, and catalytic behavior of indenyl rhodium complexes

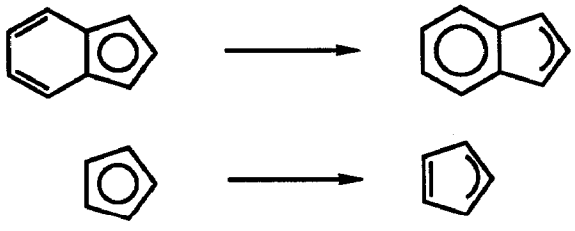

Scheme 1

[5,6,12,13], we have demonstrated [12,13] that significant slip-fold distortions, from η^5 toward η^3, exist in the ground-state structures of all d^8-[(η-C_9R_7)RhL_2] complexes; similar observations have been made by other researchers [3,14–18]. In addition, such distortions also exist for related d^6-[(η-C_9R_7)ML_2L'] systems [19,20]. The rhodium complexes all have 18-electron configurations and are best regarded as possessing "distorted η^5-"indenyl ligands.

On the basis of a comparison of the ^{13}C NMR spectra of [(η-$C_9H_7)_2Fe$], **1**, [(η-$C_9H_7)_2Co]^+$, **8**, [(η-$C_9H_7)_2Ni$], **3**, and indene, Köhler proposed [21] a correlation between the ^{13}C chemical shift of the indenyl ring junction carbons, C(3a),C(7a), and the hapticity of the coordinated indenyl ligand. Thus, the upfield shift of signals for C(3a),C(7a) in **1** and **8** relative to indene were taken as indicative of η^5-coordination, whereas the downfield shift in **3** led to the proposal of η^3-coordination for the two indenyl rings. Subsequently, Baker and Tulip [15] and our group [12,13] have analyzed the ^{13}C NMR spectra of a wide variety of indenyl metal complexes and have selected sodium indenide as a more appropriate reference. It was concluded that the solution chemical shifts for C(3a),C(7a) map the solid-state structures quite well for all d^6 and d^8 complexes examined, and that even small slip-fold distortions correlate with the ^{13}C NMR data. The publication of ^{13}C NMR spectra for the η^3-indenyl complexes **5** [9] and **6** [10] provided the first reports of such data for structurally characterized η^3-indenyls, and the values for C(3a),C(7a) were substantially downfield from those of **3** [21]. In addition, it is not necessary to invoke the presence of two η^3-indenyl ligands in **3** in order to comply with the 18-electron rule. These factors led us to propose [13] that the ground-state structure of **3** would possess either one η^3- and one η^5-indenyl ligand, cf. **7**, which must be undergoing rapid exchange in solution, or two indenyl rings with hapticities roughly halfway between true η^5- and η^3-geometries.

We therefore undertook solid-state structure determinations on **3**, the Fe and Co analogues **1** and **2**, and the permethylindenyl iron derivative **4**, in order to examine the effect of *d*-electron count on the preferred mode of coordination of the indenyl ligands. These results, and a comparison of the distortions with the analogous structurally characterized cyclopentadienyl complexes Cp_2M (Cp = (η^5-C_5H_5); M = Fe, **9** [22], Co, **10** [23], Ni, **11** [24]), [(η^5-$C_5Me_5)_2Fe$], **12** [25], and [(η^5-$C_5Me_4H)_2Fe$], **13** [26], and indenyl complexes [(η^5-$C_9H_7)_2Ru$], **14** [27], and [(η^5-1,3-$Me_2C_9H_5)_2Fe]^+$, **15** [28], are the subject of this report.

Experimental

All reactions and the growth of crystals were conducted in a nitrogen filled glove-box. The syntheses of complexes **1** [29], **2** [30], **3** [31], and **4** [32] were carried out by minor modifications of the literature procedures. Full experimental details of the modified procedures will be reported in a subsequent paper [33] along with the results of photoelectron spectroscopic and extended Hückel molecular orbital studies currently in progress. Single crystals, for X-ray diffraction analysis, were grown by cooling solutions of **1–3** (in hexane, toluene and CH_2Cl_2, respectively) to $-35\,^\circ C$ in the glove-box freezer. Crystals of **4** were grown by slow evaporation of a C_6D_6 solution at ambient temperature.

Solution ^{13}C NMR spectra were recorded in degassed C_6D_6 or CD_2Cl_2 on Bruker AC200 or AM250 spectrometers operating at 50 and 62.5 MHz respectively. Signals

Table 1

Crystal data and details of the structure determination

	Compound					
	1		2		3	4
Formula	$C_{18}H_{14}Fe$ [a]		$C_{18}H_{14}Co$		$C_{18}H_{14}Ni$	$C_{32}H_{42}Fe$
Molecular weight	286.159		289.246		289.02	482.539
Crystal system	monoclinic	monoclinic	monoclinic	monoclinic	monoclinic	orthorhombic
Cell constants						
a (Å)	8.030(2)	16.021(4)	8.027(2)	11.258(3)	6.063(1)	14.211(2)
b (Å)	7.806(2)	15.510(5)	7.838(2)	7.824(3)	20.056(3)	9.284(2)
c (Å)	10.779(2)	11.187(3)	10.936(3)	15.256(6)	10.703(2)	19.289(4)
β (°)	107.39(1)	115.53(2)	107.57(2)	108.07(2)	94.27(1)	–
Volume (Å^3)	648.9(2)	2509(1)	655.9(2)	1277.7(7)	1297.9(3)	2544.8(8)
Space group	$P2_1/n$	Cc	$P2_1/n$	$P2_1/c$	$P2_1/n$	$Pbcn$
Z	2	8	2	4	4	4
ρ_c (g cm^{-3})	1.464	1.515	1.464	1.504	1.479	1.259
F(000)	296	1184	298	596	600	1040
T (K)	295	150	295	150	150	295
μ(Mo-K_α) (cm^{-1})	11.4	11.8	12.8	13.2	14.8	5.8
Crystal size (mm)	0.19×0.29 ×0.32	0.19(100)×0.29 (021)×0.32(02$\bar{1}$)	0.44×0.47×0.50	0.44×0.47×0.50	0.39×0.41×0.46	0.42×0.50 ×0.51

Scan method	ω	$2\theta-\theta$	$2\theta-\theta$	$2\theta-\theta$	$2\theta-\theta$	ω
Scan speed (° min^{-1})	2.93–29.30	3.26–29.30	2.93–29.30	3.50–29.30	2.93–29.30	2.93–29.30
Scan width (°)	1.2	1.2 below K_{α_1} to 1.2 above K_{α_2}	1.2 below K_{α_1} to 1.2 above K_{α_2}	1.3 below K_{α_1} to 1.3 above K_{α_2}	1.2 below K_{α_1} to 1.2 above K_{α_2}	1.2
2θ Range (°)	3.5–50.0	3.5–60.0	3.5–60.0	3.5–54.0	3.5–60.0	3.5–60.0
Standard reflections	400; 004	600; 080	040; 004	1000; 0012	016, 0; 008	351; 0012
Standard variation (%)	±2	±2	±2	±2	±2	±2
Transmission factors	0.75–0.84	0.736–0.823	0.46–0.53	0.45–0.52	0.41–0.45	0.75–0.83
Unique data	1145	3694	1908	2812	3764	3701
Observed data ($I \geq 3\sigma(I)$)	890	3241	1086	2079	2441	1791
Number of variables		460		238	229	235
R ($=\Sigma\|\|F_o\|-\|F_c\|\|/\Sigma\|F_o\|$)		0.0306		0.0397	0.0413	0.0410
R_w ($=[\Sigma_w(\|F_o\|-\|F_c\|)^2/\Sigma_w\|F_o\|^2]^{1/2}$)		0.0332		0.0447	0.0493	0.0421
All data—R		0.0366		0.0535	0.0683	0.0995
All data—R_w		0.0445		0.0884	0.0719	0.0669
GoF ($=[\Sigma_w(\|F_o\|-\|F_c\|)^2/(NO-NV)]^{1/2}$)		0.96		0.84	1.37	1.36
Weighting scheme $w^{-1}=\sigma^2(F)+aF^2(a)$		0.00135		0.0094	0.00119	0.00058
Maximum residual electron density (e $Å^{-3}$)		0.72		0.75	0.72	0.35

[a] Originally reported as a 11.32(3), b 7.85(2), c 8.09(2) Å, β 115.3(5)°, space group $P2_1/a$ [34].

for the ring junction carbon atoms, C(3a),C(7a), in **1** and **3** were identified by their characteristic low intensities and by JMOD experiments. In **4**, the identification was by intensity only, as none of the ring carbons bear hydrogen substituents. The ambient temperature $^{13}C\{^1H\}$ NMR spectra for **1** and **3** agreed well with those in the literature [21,29]. A $^{13}C\{^1H\}$ NMR spectrum of **3** at $-85°C$ in CD_2Cl_2 revealed no indication of peak broadening. The $^{13}C\{^1H\}$ spectrum of **4** (C_6D_6) was not given in the original report [32] and is as follows: δ 130.6, 128.9 (s, C(4)–C(7), 85.5 (s, C(3a),C(7a)), 85.3 (s, C(7)), 70.8 (s, C(1),C(3)), 17.5, 16.9, 12.5, 10.3 (s, CH_3 groups). The intensities of the four CH_3 resonances were similar and thus, the signal due to the unique CH_3 group on C(2) could not be unambiguously identified.

Crystal data, data collection, structure solution, and refinement of 1–4

All pertinent data are listed in Table 1. Data acquisition were performed on an LT2-equipped Nicolet R3 diffractometer using graphite monochromated Mo-K_α radiation ($\lambda = 0.71073$ Å). Crystals of **2** and **3** were encased in epoxy to prevent oxidation. Accurate unit cell dimensions for each system were derived from 25 general reflections, well distributed in reciprocal space. Data collection was by either ω or 2θ–θ scan methods, with background measurements being made at the beginning and end of each scan for a total time equal to half the scan time. Two standard reflections were monitored every 100 measurements during the data collections. Absorption corrections were derived from ψ scan measurements except for **1**, which was by face-indexed analytical treatment. All structure solutions were by Patterson and Fourier techniques, and refinement was by full-matrix least-squares methods using Nicolet SHELXTLPLUS software. The atomic coordinates, bond lengths, angles, and thermal parameters are available on request from the Director of the Cambridge Crystallographic Data Centre, University Chemical Laboratory, Lensfield Rd., Cambridge CB2 1EW. Any request should be accompanied by the full literature citation for this communication.

[(η-C_9H_7)$_2$M] (M = Fe, 1; M = Co, 2)

Trotter [34] has previously determined the structure of **1** by photographic projection methods with $Z = 2$ in space group $P2_1/a$, the molecules being disordered about a center of inversion. He also noted that the structure of **2** appeared to be isomorphous with **1** based on powder data. We have indeed confirmed these observations and, although data sets for both have been collected at room temperature, no attempt has yet been made to refine these disordered structures.

However, as is not uncommonly observed for structures of spherical or ellipsoidal moieties possessing ambient temperature disorder (e.g. derivatives of adamantane and related species [35]), both **1** and **2** undergo phase transitions to give ordered low-temperature forms. Although clearly isostructural at 295 K, the similarities are lost below ~ 240–245 K. The first low-temperature attempt on **2** was performed by slow cooling of the crystal down to 150 K. This data set yielded a result indicating an incomplete change with ~ 15% residual disorder. A second experiment involved maintaining the temperature at 233 K for 16 hours prior to final cooling. Although a much more complete transformation was achieved, 4% residual disorder remained. The $P2_1/n$ ($Z = 2$) to $P2_1/c$ ($Z = 4$) transition of **2** is not duplicated by **1**, which gave a low temperature C-centered monoclinic cell with $Z = 8$. Again, the crystal was maintained at 233 K for 16 hours prior to final cooling to 150 K. Initial

attempts to solve **1** in $C2/c$ proved inappropriate, but solution and refinement was successful in Cc, with two independent molecules per asymmetric unit. E statistics also strongly favored the acentric solution. Again, the phase transformation was incomplete, but only ~ 2% disorder remained for **1**. Inversion of the coordinates of **1** gave slightly poorer agreement factors ($R = 0.0316$, $R_w = 0.0339$), so the setting chosen is assumed correct. The residual metal atom disorder was included in the refinements of both **1** and **2**. However, the corresponding indenyl carbon atoms (which exhibited peak heights ~ 0.25 e $Å^{-3}$, considerably less than the ordered-form hydrogen atoms) were not included.

[(η-C_9H_7)$_2$Ni], 3

Of the three low-temperature structure experiments, only **3** did not exhibit any phase change over the temperature range studied (150–295 K). Numerous crystals were mounted and examined, but most showed photographic evidence of almost parallel twinning. Although the crystal utilized for the data collection did not show this effect, the highly anisotropic thermal parameters exhibited by certain atoms in the structure are presumably due to some twinning phenomenon. Data sets were collected from two additional "good" crystals; however, similar anisotropies were observed in the thermal parameters for the same carbon atoms and slightly poorer agreement factors were obtained.

[(η-C_9Me_7)$_2$Fe], 4

The structure of **4** was only examined at 295 K, and solved and refined routinely. The molecule possesses two-fold crystallographic symmetry.

Results and discussion

Solid-state structures of [(η-C_9H_7)$_2$Fe], 1, and [(η-C_9Me_7)$_2$Fe], 4

Solution ^{13}C NMR data for the iron complexes **1** and **4** (Table 2) are indicative of nearly perfect η^5-coordination of the indenyl ligands. Crystallographic disorder in **1** at room temperature limits the accuracy of this result; however, we observed that the crystal underwent a non-destructive phase transition at ca. 245 K, below which an essentially ordered results was obtained. Only ca. 2% residual disorder remained at 150 K but there were two independent molecules in the asymmetric unit.

We have chosen [12,13,15] several parameters to describe the slip-fold distortion in indenyl complexes. First, we define Δ_{M-C}, the slip parameter, as the difference in the average bond lengths of the metal to the ring junction carbons C(3a),C(7a) and the metal to the adjacent carbon atoms of the five-membered ring, C(1),C(3). Secondly, we define the hinge angle, HA, as the angle between the planes [C(1),C(2),C(3)] and [C(1),C(3),C(3a),C(7a)], and the fold angle, FA, as the angle between the planes [C(1),C(2),C(3)] and [C(3a),C(4),C(5),C(6),C(7),C(7a)]. The hinge angle represents bending at [C(1),C(3)] whereas the fold angle takes into account a smaller bending distortion at C(3a),C(7a). Although other workers [19] have selected different, but related, parameters to describe these distortions, Δ_{M-C} values can always be obtained in a straightforward manner from tabulated bond lengths, and FA is usually reported. For the sandwich complexes, it was necessary to select an additional parameter to describe the relative rotational orientation of the two indenyl rings. We define the rotation angle, RA, as the angle between planes

Table 2

Comparison of solid state structural and solution ^{13}C NMR data for indenyl complexes

Compound	No.	Solvent	δ $^{13}C(3a),^{13}C(7a)$	$\Delta\delta^{13}C$ [a]	Δ_{M-C} (Å) [b]		Avg. (M–C) (Å)	HA (°) [c]		FA (°) [d]		RA (°) [e]	Ref.
$[(\eta\text{-}C_9H_7)_2Fe]$	1	C_6D_6	87.0	−43.7	0.0495	0.0495		2.6	2.6	0.4	1.6	13.0	f
					0.0335	0.0385		2.1	1.6	0.9	0.4	5.2	
					Avg.	0.043(4)	2.065(4)	2.2		0.8			
$[(\eta\text{-}C_9Me_7)_2Fe]$	4	C_6D_6	85.5	−38.3	0.030(4)		2.074(4)	2.5		4.4		151.3	f
$[(\eta\text{-}C_9Me_2H_5)_2Fe]^+$	5	–	–	–	0.074(4)		2.103(4)	–		–		–	28
$[(\eta\text{-}C_9H_7)_2Ru]$	14	$CDCl_3$	89.9	−40.8	0.030(14)		2.190(14)	ca. 0		ca. 0		ca. 0	27
$[(\eta\text{-}C_9H_7)_2Co]^+$	8	$(CD_3)_2CO$	98.3	−32.4	–		–	–		–		–	21
$[(\eta\text{-}C_9H_7)_2Co]$	2	–	–	–	0.114	0.134		7.3	7.8	6.0	5.9	10.7	f
					Avg.	0.124(4)	2.121(4)	7.6		6.0			
$[(\eta\text{-}C_9H_7)_2Ni]$	3	C_6D_6	134.3	+3.6	0.419	0.416		13.7	14.1	12.7	13.4	175.0	f
					Avg.	0.418(6)	2.204(6)	13.9		13.1			
$[(\eta\text{-}C_9H_7)Ir(PMe_2Ph)_3]$	5	C_6D_6	156.4	+25.7	0.79(1)		–	–		28		–	9
$[(\eta\text{-}C_9H_7)Fe(CO)_3]^-$	6	CD_3CN	157.3	+26.6	0.689(7)		–	–		22		–	10
$[(\eta\text{-}C_9H_7)_2W(CO)_2]$	7	–	–	–	0.07(2) [g]		–	–				–	11
					0.72(2) [h]					26			
$[(\eta\text{-}C_9H_7)_2V(CO)_2]$	16	–	–	–	0.120(3) [g]		–	–				–	38
					0.493(3)					12			

[a] $\Delta\delta^{13}C = \delta\ ^{13}C(3a),^{13}C(7a)$ (η-indenyl) $- \delta\ ^{13}C(3a),^{13}C(7a)$ (Na^+ [indenyl]$^-$). [b] Δ_{M-C} = [average of M–C(3a),C(7a)] − [average of M–C(1),C(3)]. [c] HA = hinge angle = angle between planes [C(1),C(2),C(3)] and [C(1),C(3),C(3a),C(7a)]. [d] FA = fold angle = angle between planes [C(1),C(2),C(3)] and [C(3a),C(4),C(5),C(6),C(7),C(7a)]. [e] RA = Rotation angle = angle between planes defined by [M,C(2),mid C(3a),C(7a)] and [M,C(2), mid C(3a'),C(7a')]. For compounds 3 and 4, the complement of this angle is given. [f] This work. [g] η^5-Indenyl ring. [h] η^3-Indenyl ring.

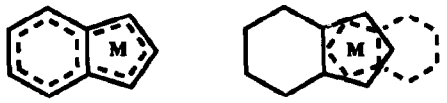

RA = 0° RA = 180°

Scheme 2

including the metal, and C(2) and the midpoint of C(3a),C(7a) for each of the indenyl rings, i.e. [M,C(2),mid C(3a),C(7a)] and [M,C(2′),mid C(3a′),C(7a′)]. A rotation angle of 0° would indicate a completely eclipsed geometry whereas an angle of 180° corresponds to the fully staggered arrangement of the two rings (Scheme 2).

The values of Δ_{M-C}, HA, FA, and RA are given in Table 2. The structure of **1** is illustrated in Fig. 1. Bond lengths for **1–4** and **15** are given in Table 3. The values of Δ_{M-C}, FA and HA for the two independent molecules in the asymmetric unit of **1** are all small and essentially similar (average values are 0.043(4) Å, 2.2°, and 0.8°, respectively). These values correspond to nearly undistorted η^5-coordination of both

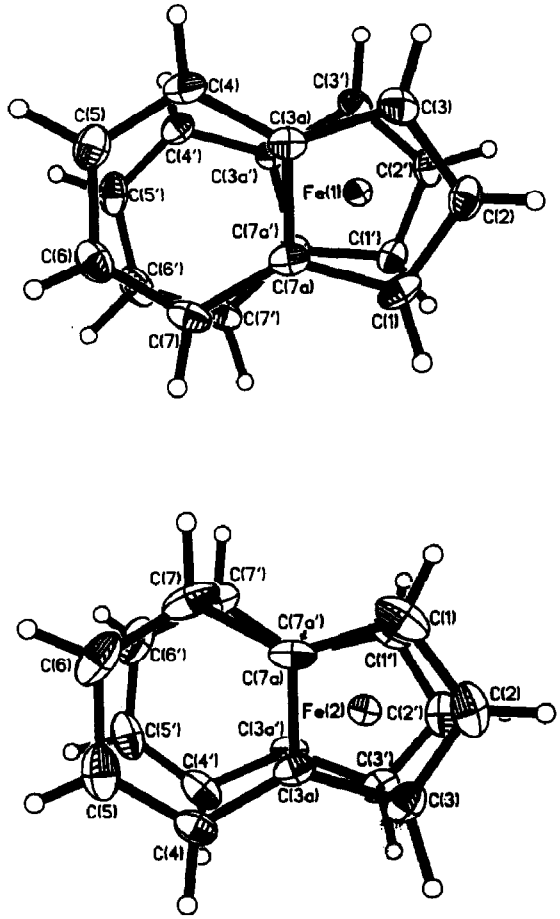

Fig. 1. ORTEP views of $[(\eta\text{-}C_9H_7)_2Fe]$, **1**, molecule A (top) and B (bottom), showing atom numbering.

Table 3

Bond lengths for indenyl sandwich compounds of Fe, Co, and Ni

	1		2	3	4	15 [a]
	Molecule A	Molecule B				
M–C(1)	2.047(3)	2.045(4)	2.080(3)	2.068(3)	2.058(4)	2.079(4)
M–C(2)	2.041(3)	2.045(4)	2.090(4)	1.973(3)	2.063(4)	2.063(4)
M–C(3)	2.049(4)	2.054(4)	2.059(3)	2.056(3)	2.066(3)	2.073(4)
M–C(3A)	2.101(4)	2.087(4)	2.181(3)	2.480(3)	2.086(4)	2.142(4)
M–C(7A)	2.094(4)	2.079(4)	2.186(2)	2.483(3)	2.098(4)	2.156(4)
M–C(1′)	2.042(4)	2.052(5)	2.058(3)	2.056(4)	*	2.076(4)
M–C(2′)	2.034(4)	2.048(5)	2.086(3)	1.978(6)	*	2.070(4)
M–C(3′)	2.054(4)	2.049(4)	2.072(3)	2.029(5)	*	2.072(4)
M–C(3a′)	2.103(3)	2.087(3)	2.195(3)	2.462(3)	*	2.151(4)
M–C(7a′)	2.092(3)	2.091(3)	2.204(3)	2.455(3)	*	2.147(4)
C(1)–C(2)	1.419(5)	1.421(5)	1.413(4)	1.408(5)	1.427(6)	1.409(6)
C(2)–C(3)	1.434(6)	1.420(7)	1.411(5)	1.414(5)	1.412(5)	1.417(6)
C(3)–C(3a)	1.439(5)	1.437(5)	1.444(4)	1.458(4)	1.455(5)	1.439(6)
C(3a)–C(7a)	1.455(5)	1.450(5)	1.439(4)	1.425(4)	1.446(5)	1.446(6)
C(7a)–C(1)	1.431(7)	1.434(8)	1.460(4)	1.454(4)	1.437(5)	1.438(6)
C(3a)–C(4)	1.435(6)	1.419(6)	1.418(5)	1.390(4)	1.437(5)	1.411(6)
C(4)–C(5)	1.358(5)	1.360(5)	1.370(4)	1.391(4)	1.365(5)	1.352(7)
C(5)–C(6)	1.426(6)	1.433(6)	1.411(5)	1.393(5)	1.456(5)	1.420(8)
C(6)–C(7)	1.357(7)	1.349(8)	1.365(5)	1.385(4)	1.368(5)	1.360(7)
C(7)–C(7a)	1.432(5)	1.426(6)	1.407(3)	1.404(4)	1.440(5)	1.422(6)
C(1′)–C(2′)	1.431(4)	1.431(5)	1.427(4)	1.398(8)	*	1.420(6)
C(2′)–C(3′)	1.431(6)	1.415(7)	1.419(4)	1.367(12)	*	1.421(6)
C(3′)–C(3a′)	1.441(4)	1.431(5)	1.463(4)	1.468(6)	*	1.452(6)
C(3a′)–C(7a′)	1.449(5)	1.456(5)	1.445(4)	1.418(5)	*	1.424(6)
C(7a′)–C(1′)	1.441(5)	1.434(6)	1.448(4)	1.445(5)	*	1.441(6)
C(3a′)–C(4′)	1.421(6)	1.430(7)	1.404(4)	1.395(5)	*	1.406(6)
C(4′)–C(5′)	1.356(5)	1.356(6)	1.365(4)	1.386(7)	*	1.360(8)
C(5′)–C(6′)	1.423(6)	1.432(7)	1.406(5)	1.363(6)	*	1.409(8)
C(6′)–C(7′)	1.354(6)	1.358(8)	1.377(5)	1.361(5)	*	1.376(8)
C(7′)–C(7a′)	1.431(4)	1.419(5)	1.408(4)	1.391(4)	*	1.414(6)

[a] From ref. 28. * Symmetry related.

indenyl rings, consistent with the solution ^{13}C NMR data, and with an 18-electron count at iron. Interestingly, the values for RA, 13.0 and 5.2°, are significantly different, indicating a soft energy surface for at least partial ring rotation in these compounds. Both values are, however, relatively small. The corresponding RA for ferrocene, in its low temperature triclinic form, is 9° [22].

The ^{13}C NMR spectrum of the permethylindenyl derivative **4** was also indicative of a relatively undistorted η^5-structure. Consistent with this observation, the solid state results give $\Delta_{M-C} = 0.030(4)$ Å, HA = 2.5°, and FA = 4.4°, quite similar to those for **1** and its ruthenium analogue [$(\eta$-$C_9H_7)_2Ru$], **14** [27]. Unlike **1** and **14**, however, the RA for **4** is 151.3° (Fig. 2), which represents an alternative eclipsed geometry. This result was somewhat surprising in light of the fact that [$(\eta^5$-$C_5Me_5)_2Fe$], **12**, exhibits the staggered D_{5d} geometry in the solid state [25]. Clearly, steric interactions between methyl groups on the two rings are not a significant factor in determining the solid state structure of **4**. In addition, permethylation of

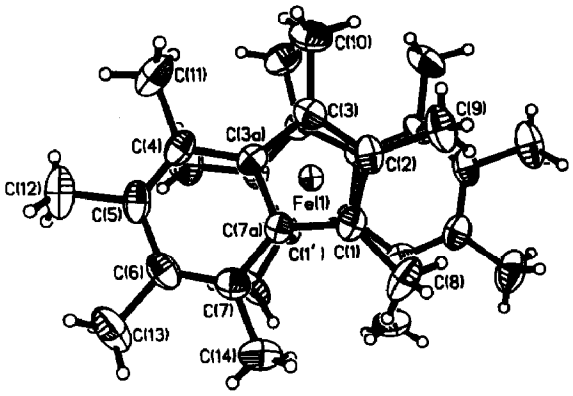

Fig. 2. ORTEP view of $[(\eta\text{-}C_9Me_7)_2Fe]$, **4**, showing atom numbering.

the indenyl rings does not influence the degree of slip-fold distortion in **4** vs. **1**, consistent with our previous observations for $[(\eta\text{-}C_9R_7)Rh(\eta\text{-}1,5\text{-COD})]$ (R = H, Me) [13].

Bond lengths for the 17-electron analogue $[(\eta\text{-}1,3\text{-}Me_2C_9H_5)_2Fe]^+$, **15** [28], (Table 3) and $\Delta_{M-C} = 0.074(4)$ Å (Table 2), indicate a slight increase in slippage for **15** vs. **1** and **4**. The average M–C(1),C(3) (**1** = 2.049(4), **4** = 2.062(4), **15** = 2.075(4) Å), M–C(2) (**1** = 2.042(5), **4** = 2.063(4), **15** = 2.067(4) Å), and M–C(3a),C(7a) (**1** = 2.092(4), **4** = 2.092(4), **15** = 2.149(4) Å) distances indicate the similarity between **1** and **4** (avg. M–C = 2.065(4) and 2.074(4) Å, respectively) and a significant increase in all M–C distances for **15** (avg. M–C = 2.103(4) Å). The reasons for the increases in **15** are not clear at present; the results of a combined PES and EHMO study [36] on **1** indicate that the top three filled levels are largely metal in character. In any event, the distortions in M–C bonding in **15** are relatively small compared with those in **2** and **3**, see below.

Solid state structure of $[(\eta\text{-}C_9H_7)_2Co]$, 2

The cobalt complex **2** is paramagnetic, with a formal electron count of 19, and thus slippage cannot be inferred directly from the ^{13}C NMR resonances for C(3a),C(7a) due to paramagnetic contact shifts. We therefore carried out a single-crystal X-ray diffraction study on this compound. As we observed for **1**, see above, **2** is also disordered at ambient temperatures. Initially, we cooled the crystal to 150 K and observed a non-destructive phase change from $P2_1/n$, $Z = 2$, to $P2_1/c$, $Z = 4$. Solution of this data yielded an 85/15% disorder, and we considered the possibility that the phase change was "incomplete". Upon warming the crystal to room temperature, the original $P2_1/n$, $Z = 2$ cell was obtained, indicating that the transition was reversible. We then cooled the crystal slowly, and diffraction evidence indicated that a significant change was taking place at ca. 240 K. The crystal was kept at ca. 233 K for 16 hours and then cooled to 150 K. The new data set indicated only ca. 4% residual disorder. The structural parameters reported in Tables 2 and 3, and the ORTEP diagram (Fig. 3), are from this solution. It seems possible that a completely ordered structure might be obtained if the cooling was sufficiently slow.

As expected, the presence of an additional electron in **2** vs. **1** results in an increase in the degree of slip-fold distortion of the indenyl rings. Parameters for the two chemically equivalent but crystallographically distinct indenyl rings are quite

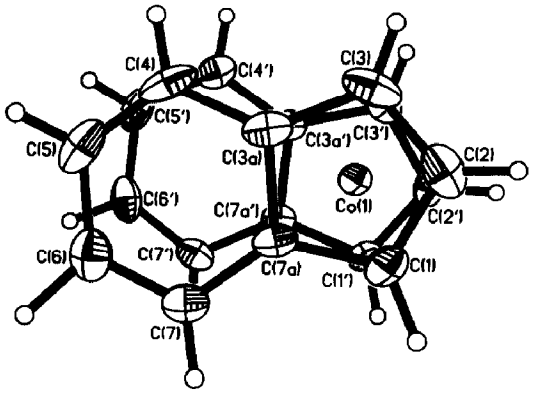

Fig. 3. ORTEP view of $[(\eta\text{-}C_9H_7)_2Co]$, **2**, showing atom numbering.

similar, with average values of $\Delta_{M-C} = 0.124(4)$ Å, HA = 7.6°, and FA = 6.0°. These values are at the low end of the range observed for $[(\eta\text{-}C_9R_7)RhL_2]$ complexes, e.g. $\Delta_{M-C} = 0.112(2)$–$0.227(3)$ Å [37]. The rotation angle, RA = 10.7°, is in between the values for the two independent molecules of **1**. and is close to the fully eclipsed values. The average M–C distance (Table 2) for **2**, 2.121 (4) Å (average of 10 Co–C distances) is significantly larger than that for **1**, 2.065(4) Å (average of 20 Fe–C distances). The largest difference is observed in the average M–C(3a),C(7a) distances of 2.192(3) for **2**, and 2.092(4) for **1**. Clearly, **2** should be regarded as having "distorted η^5-"coordination of the two indenyl rings.

Solid state structure of $[(\eta\text{-}C_9H_7)_2Ni]$, 3

Complex **3** is known to be diamagnetic [31], in contrast to $[(\eta^5\text{-}C_5H_5)_2Ni]$, **11**, which has two unpaired electrons. The previously reported [21] ^{13}C NMR study on **3** led to the proposal by Köhler that both indenyl rings were coordinated in an η^3-fashion, leading to a 16-electron count at Ni. This report [21], which suggested that indenyl hapticity correlates with the ^{13}C NMR chemical shift of the ring junction carbons C(3a),C(7a) was based on a comparison of NMR data for **1**, **8**, **3**, and indene. We [12,13] and others [9,15] have analyzed the ^{13}C NMR spectra of a large number of indenyl complexes of d^6 and d^8 metals, and find that there is a strong correlation between the solid state structure parameter Δ_{M-C} and δ $^{13}C(3a)$,$^{13}C(7a)$. Much of the available data were illustrated graphically in reference [15]. Other researchers have been developing additional correlations between Δ_{M-C} and differences in the ^{13}C or ^{1}H NMR chemical shifts for C(1),C(3) vs C(2) [18], or H(1,3) vs. H(2) [9]. Köhler's assessment of **3** was made prior to the structural or ^{13}C NMR characterization of the η^3-complexes **5**, **6** and **7**, which have Δ_{M-C} values of 0.79(1), 0.689(7), and 0.72(2) Å, respectively, for the η^3-indenyl rings. The solid state values of FA for the η^3-indenyl ligands in **5**, **6** and **7** are 28, 22 and 26°, respectively; HA values were not reported. The ^{13}C NMR data for **5** and **6** indicate that C(3a),C(7a) resonate at 156.4 and 157.3 ppm, respectively, over 20 ppm downfield from **3**. No ^{13}C NMR data were obtained for **7** due to limited solubility [11]. Interestingly, **7** contains both η^5- and η^3-indenyl rings in the solid state (Δ_{M-C} for $\eta^5\text{-}C_9H_7 = 0.07(2)$ Å), although it was suggested that the two rings might be undergoing rapid exchange in solution.

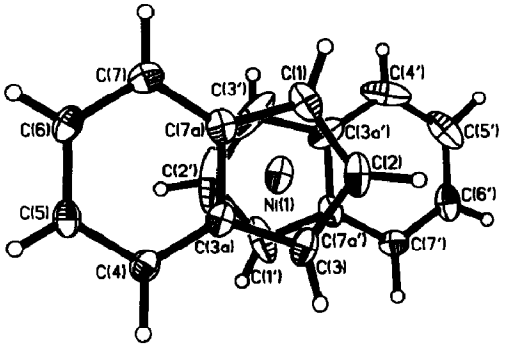

Fig. 4. ORTEP view of $[(\eta\text{-}C_9H_7)_2Ni]$, **3**, showing atom numbering. The view selected is in the mean plane of [C(1),C(3a),C(7a),C(3)].

The large difference in the chemical shifts of C(3a),C(7a) for **3** vs. **5–7** led us to propose [13] two alternative possibilities for **3**, namely that either an analogous situation to **7** exists in which the η^5- and η^3-rings would be in rapid equilibrium, or that both indenyl rings exhibited an intermediate degree of distortion, approximately half-way between η^5- and η^3-geometries. A ^{13}C NMR spectrum of **3** was recorded at $-85\,^\circ C$, on a 250 MHz spectrometer; however, only five sharp peaks were observed for the indenyl carbon atoms, identical to those observed at ambient temperature. Thus, for a dynamic process to be occurring, the barrier must be extremely small.

There is only one reported [38] structure of an indenyl complex which displays an intermediate Δ_{M-C} value of 0.493(3) Å for an indenyl ring. This is the paramagnetic species $[(\eta\text{-}C_9H_7)_2V(CO)_2]$, **16**, in which the other indenyl ring has a Δ_{M-C} of 0.120(3) Å. The intermediate value of 0.493(3) Å may be a reflection of the formal 17- or 19-electron counts, which would be obtained by true η^3- or η^5-coordination of this indenyl ligand. Similar to the tungsten analogue **7**, and in contrast to **2**, the distortion in **16** appears to be localized in one indenyl ring.

After several attempts, we obtained an adequate X-ray data set for **3** at 150 K. Two views of **3** are given in Fig. 4 and 5. The large anisotropy for certain carbon atoms in one of the indenyl rings is probably associated with some form of twinning (see Experimental). However, the structure is certainly of sufficient accuracy to demonstrate the important points concerning indenyl hapticity. Although the two indenyl ligands are crystallographically distinct, the slip parameters, Δ_{M-C}, and fold parameters, HA and FA, are quite similar, with average values of 0.418(6) Å, 13.9°, and 13.1°, respectively. Thus, both ring systems are equally distorted away from η^5-coordination, ca. half-way to η^3-bonding modes. The solid-state result is entirely consistent with the low temperature ^{13}C NMR study, and contrasts with the structure of **7** and **16**, and with the initially proposed structure of Köhler. Also of interest is the value of RA = 175.0°, indicating a nearly fully staggered geometry.

The average of all 10 Ni–C contacts is 2.204(6) Å, significantly larger than in either **1**, **2**, or **4**. Whereas the average value of Ni–C(1),C(3) of 2.052(5) Å is similar to those in **1**, 2.049(4) Å, and **2**, 2.067(3) Å, the average Ni–C(2) distance, 1.976(6) Å, is unusually short (cf. **1** = 2.042(5), **2** = 2.088(4) Å), and the average Ni–C(3a),C(7a) distance of 2.470(3) Å is unusually long (**1** = 2.092(4), **2** = 2.192(3) Å). The structure of the cyclopentadienyl nickel allyl complex $[(\eta^5\text{-}C_5H_5)Ni(\eta^3,\eta^3\text{-}2,2'\text{-}$

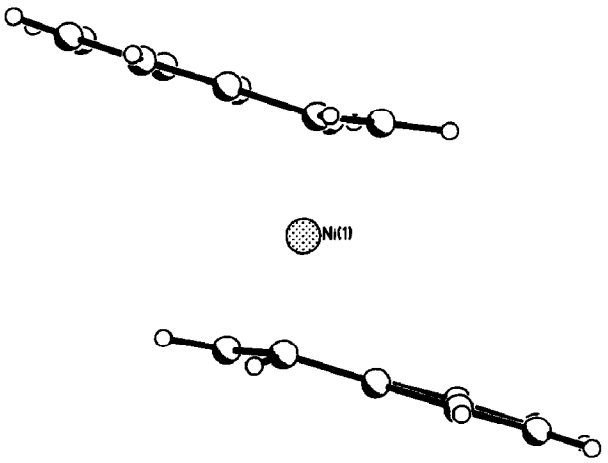

Fig. 5. Ball and stick view of [(η-C_9H_7)$_2$Ni], 3, with the plane [C(1),C(2),C(3)] perpendicular to the page. The hinge angle, HA, is clearly visible, as is the slip-displacement of Ni.

$C_3H_4C_3H_4$)Ni(η^5-C_5H_5)], 17, has been reported [39]. The average Ni–terminal allyl carbon distance of 1.972(4) Å and Ni–central allyl carbon distance of 1.933(3) Å in this species are both significantly shorter than the Ni–C(1),C(3) and Ni–C(2) distances in 3, providing additional evidence that 3 is not a "true η^3-"complex.

Comparison of indenyl C–C bond lengths in 1–4

As stated in the Introduction, slip-fold distortions of the indenyl ring away from η^5- towards η^3-coordination are expected to result in a rehybridization of the 10-π aromatic system of the indenyl moiety. Figure 6 displays the C–C bond distances in 1–4. In this figure, all chemically related values have been averaged, except for C(1)–C(2) and C(2)–C(3) in 3, for which only the values for the better behaved ring were used. Complete listings of all C–C bond lengths with esd's are given in Table 3. As can be seen from Table 3, the esd's for the C–C distances used in Fig. 6 range from 0.004 to 0.008 Å, most falling in the range of 0.004–0.006 Å. Several trends are apparent which deserve comment. There is clearly a butadiene-like variation in the C–C distances in the 6-membered rings in 1 and 4, with C(4)–C(5) and C(6)–C(7) being significantly shorter than the remaining C–C distances. As the degree of slip-fold distortion increases on going from 1 to 3, C(4)–C(5) increases to 1.381 Å, and C(3a)–C(4), C(5)–C(6) and C(3a)–C(7a) decrease to 1.396, 1.378, and 1.422 Å, respectively, in 3. Thus, the distances within the 6-membered ring, with the exception of the ring junction C(3a)–C(7a), are similar and close to the value of 1.935 Å for benzene. The C(3)–C(3a) distances increase in the order 1 (1.436 Å), 2 (1.454 Å), 3 (1.456 Å), and the C(2)–C(3) distances decrease in the order 1 (1.425 Å), 2 (1.418 Å), 3 (1.411 Å), also reflecting the gradual localization of the allylic moiety C(1),C(2),C(3). The latter distance is similar to the average allyl C–C distance of 1.410(6) Å in the CpNi-allyl complex 17 [39]. Thus, the data are of sufficient quality to demonstrate the trends in C–C distances consistent with a gradual increase in aromaticity of the 6-membered ring and localliization of the allylic moiety of the 5-membered ring, as the slip-fold distortion increases. Note that in the η^3-complex 6 [10], however, the C(3a)–C(7a) distance is 1.397(6) Å, significantly shorter than that in 3. This is consistent with the fact that 3 is not a "true η^3-"complex.

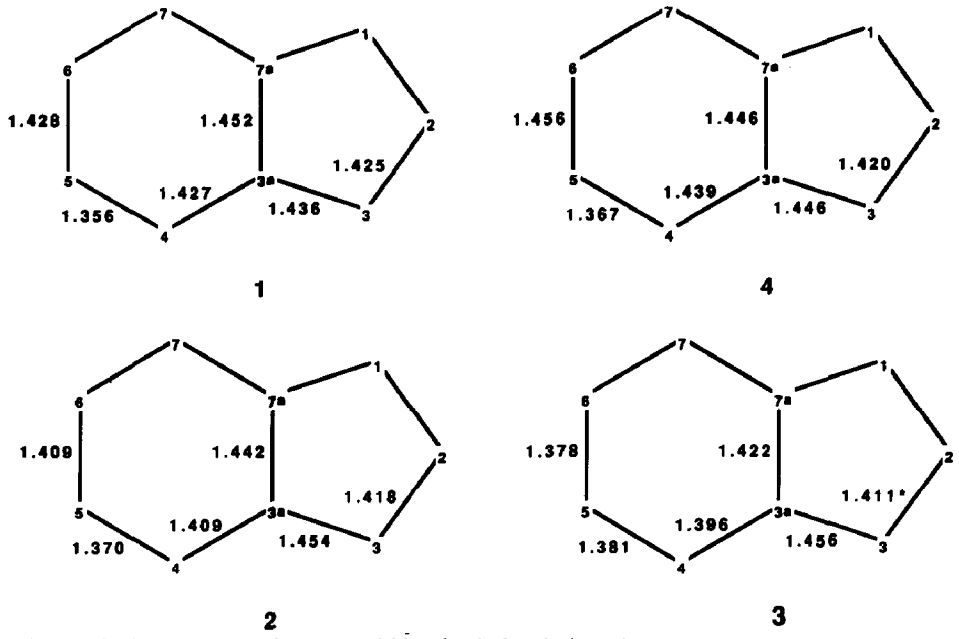

Fig. 6. Carbon–carbon distances within the indenyl rings in **1–4**. Distances are the average of all chemically related bonds, except for C(2)–C(3) in **3**, which is the average of C(1)–C(2) and C(2)–C(3) for the better-behaved indenyl ring (i.e. (C(1′)–C(2′) and C(2′)–C(3′) were not included in the calculation).

Comparison with solid state structures of [Cp_2M] complexes

It is interesting to compare the solid-state structures of **1–4** with those of the analogous cyclopentadienyl species [(η^5-C_5H_5)$_2$M] (M = Fe, **9** [22], Co, **10** [23], Ni, **11** [24]), and their methyl substituted derivatives [(η^5-C_5Me_5)$_2$Fe], **12** [25], and [(η^5-C_5Me_4H)$_2$Fe], **13** [26]. The cyclopentadienyl complexes all exhibit nearly perfect five-fold symmetry in the solid state; average M–C distances are given in Table 4. The values for the iron compounds **9**, **12**, and **13** are identical within 3 esd's. The addition of electrons into the doubly degenerate M-ring antibonding level results in a gradual expansion of the sandwich along the five-fold rotational axis.

The highest order rotational axis in the indenyl sandwiches is of order 2, which implies a lack of degeneracy in any of the molecular orbital levels. This is clearly observed by the diamagnetism of **3**. Extended Hückel molecular orbital calculations and photoelectron spectra for **1** and **14** have been reported [36], and similar studies of **2**, **3**, and **4** are currently in progress [33]. It is clear, however, that the distortions in the indenyl complexes are fundamentally different than those exhibited by their

Table 4

Comparison of average M–C distances in Cp_2M compounds

Compound	No.	Average M–C (Å)	Ref.
(η^5-C_5H_5)$_2$Fe	**9**	2.046(2)	22
(η^5-C_5Me_5)$_2$Fe	**12**	2.050(2)	25
(η^5-C_5Me_4H)$_2$Fe	**13**	2.054(3)	26
(η^5-C_5H_5)$_2$Co	**10**	2.119(3)	23
(η^5-C_5H_5)$_2$Ni	**11**	2.185(4)	24

cyclopentadienyl analogues, and that this is due to the lower symmetry and lack of degeneracy of the π-orbitals on the indenyl ligands. It is intriguing that the average M–C contacts in **1–3** are reasonably close to those in their (η-C_5H_5) analogues **9–11**, respectively. Whether this fact is of any fundamental significance is not clear. It is also not clear why the rotational preferences differ so much for **1–4**. We hope to answer some of these questions with the aid of EHMO calculations [33].

Conclusions

The crystal and molecular structures of a series of indenyl sandwich complexes, [(η-C_9H_7)$_2$M (M = Fe, **1**; Co, **2**; Ni, **3**) and [(η-C_9Me_7)$_2$Fe], **4**, have been determined by single-crystal X-ray diffraction methods. Slip-fold distortions are extremely small for the 18-electron complexes **1** and **4**, consistent with the ^{13}C NMR chemical shifts of the ring junction carbons. The two structures differ in that, in **1**, the indenyl rings are almost completely eclipsed with the 6-membered rings within 5.2 or 13.0° of being superimposable in the two independent molecules, whereas, in **4**, the rings are rotated by 151.3° with respect to each other yielding an alternative eclipsed geometry. The cobalt complex **2** has one additional electron, resulting in a modest slip-fold distortion of both rings toward an η^3-geometry. The ring systems are rotated by 10.7° with respect to a fully eclipsed geometry. The nickel complex **3** avoids an unfavorable 20-electron count by significant slip-fold distortion of both indenyl rings. The average values of Δ_{M-C} (0.418(6) Å), the hinge angle (13.9°), and fold angle (13.1°) for **3** are half-way between those for true η^5- and η^3-coordination modes. This demonstrates the flexibility of indenyl ligands, in that a wide variety of electron counts can be stabilized by gradual slip-fold distortions. As the indenyl rings in **1–3** gradually approach η^3-coordination, the π-system rehybridizes to increase aromaticity in the 6-membered ring and localizes the allylic portion of the 5-membered ring. This is evidenced by changes in the C–C bond lengths in the three structures.

The availability of a wide range of intermediate hapticities between η^5- and η^3-distinguishes indenyl ligands from their cyclopentadienyl analogues. For example, in the Cp_2M complexes (M = Fe, Co, Ni) **9–11**, five-fold rotational symmetry is maintained throughout the series, with additional electrons above the 18-count for Cp_2Fe resulting in a gradual expansion of the complexes along the five-fold axis.

A correlation between indenyl hapticity and the position of the ^{13}C NMR shifts for the ring junction carbons C(3a),C(7a) initially proposed by Köhler [21] led him to suggest that **3** contained two η^3-indenyl rings. Although this is not the correct structure for **3**, additional ^{13}C NMR data on structurally characterized η^3-indenyl complexes, combined with the data presented in this report, demonstrate the fundamental validity of the correlation and the fact that it can be used to predict accurately the degree of slip-fold distortion anywhere between "true η^5-" and "true η^3-"geometries.

Studies of the photoelectron spectra and extended Hückel molecular orbital calculations on **1–4** are currently in progress and will be reported in due course [33].

Acknowledgment

TBM thanks the Natural Sciences and Engineering Research Council of Canada, Imperial Oil Ltd. (Canada), and the Donors of the Petroleum Research Fund

administered by the American Chemical Society, for support, the DuPont Company (U.S.A.) for a generous donation of materials and supplies, Dr. S. Collins for assistance with the synthesis of heptamethylindene, L. Koch for translation of several references, and A. Brunelle for assistance with the preparation of the manuscript.

References

1 For a review, see: J.M. O'Connor and C.P. Casey, Chem. Rev., 87 (1987) 307, and references therein.
2 C. White and R.J. Mawby, Inorg. Chim. Acta, 4 (1970) 261; C. White, R.J. Mawby and A.J. Hart-Davis, ibid., 4 (1970) 441; D.J. Jones and R.J. Mawby, ibid., 6 (1972) 157; N.N. Turaki, J.M. Huggins and L. Lebioda, Inorg. Chem., 27 (1988) 424.
3 P. Caddy, M. Green, E. O'Brien, L.E. Smart, and P. Woodward, J. Chem. Soc., Dalton Trans., (1980) 962; Angew. Chem., Int. Ed. Engl., 16 (1977) 648.
4 M.E. Rerek and F. Basolo, J. Am. Chem. Soc., 106 (1984) 5908; L.-N. Ji, M.E. Rerek and F. Basolo, Organometallics, 3 (1984) 740; M.E. Rerek, L.-N. Ji and F. Basolo, J. Chem. Soc., Chem. Commun., (1983) 1208; A.J. Hart-Davis and R. Mawby, J. Chem. Soc. A, (1969) 2403.
5 T.B. Marder and I.D. Williams, J. Chem. Soc., Chem. Commun., (1987) 1478; A.K. Kakkar, N.J. Taylor and T.B. Marder, Organometallics, 8 (1989) 1765.
6 T.B. Marder, D.C. Roe and D. Milstein, Organometallics, 7 (1988) 1451.
7 P. Caddy, M. Green, L.E. Smart and N. White, J. Chem. Soc., Chem. Commun., (1978) 839; A. Borrini, P. Diversi, G. Ingrosso, A. Lucherini and G. Serra, J. Mol. Catal., 30 (1985) 181.
8 H. Bonneman, Angew. Chem., Int. Ed. Engl., 24 (1985) 248; H. Bonneman and W. Brijoux in: R. Ugo (Ed.), Aspects of Homogeneous Catalysis, Vol. 5, D. Reidel, Dordrecht, 1984, p. 75.
9 J.S. Merola, R.-T. Kacmarcik and D. Van Engen, J. Am. Chem. Soc., 108 (1986) 329.
10 T.C. Forschner, A.R. Cutler and R.K. Kullnig, Organometallics, 6 (1987) 889.
11 A.W. Nesmeyanov, N.A. Ustynyuk, L.G. Makarova, V.G. Andrianov, Yu.T. Struchkov, S. Andrae, Yu.A. Ustynyuk and S.G. Malyugina, J. Organomet. Chem., 159 (1978) 189.
12 T.B. Marder, J.C. Calabrese, D.C. Roe and T.H. Tulip, Organometallics, 6 (1987) 2012; R.T. Carl, R.P. Hughes, A.L. Rheingold, T.B. Marder and N.J. Taylor, ibid., 7 (1988) 1613; A.K. Kakkar, N.J. Taylor, J.C. Calabrese, W.A. Nugent, D.C. Roe, E.A. Connaway and T.B. Marder, J. Chem. Soc., Chem. Commun., (1989) 990.
13 A.K. Kakkar, S.F. Jones, N.J. Taylor, S. Collins and T.B. Marder, J. Chem. Soc., Chem. Commun., (1989) 1454.
14 M. Mlekuz, P. Bougeard, B.G. Sayer, M.J. McGlinchey, C.A. Rodger, M.R. Churchill,, J.W. Ziller, S.-W. Kanz and T.A. Albright, Organometallics, 5 (1986) 1656.
15 R.T. Baker and T.H. Tulip, Organometallics, 5 (1986) 839.
16 Y.N. Al-Obaidi, P.K. Baker, M. Green, N.D. White and G.E. Taylor, J. Chem. Soc., Dalton Trans., (1981) 2321.
17 (M = Ir) J.S. Merola, personal communication to T.B.M.; see also: J.S. Merola and R.T. Kacmarcik, Organometallics, 8 (1989) 778.
18 A. Ceccon, A. Gambaro, S. Santi, G. Valle and A. Venzo, J. Chem. Soc., Chem. Commun., (1989) 51.
19 J.W. Faller, R.H. Crabtree and A. Habib, Organometallics, 4 (1985) 929.
20 A.K. Kakkar, N.J. Taylor and T.B. Marder, unpublished results.
21 F.H. Köhler, Chem. Ber., 107 (1974) 570.
22 J.D. Dunitz, L.E. Orgel and A. Rich, Acta Crystallogr., 9 (1956) 373; for low temperature redetermination, see: P. Seiler and J.D. Dunitz, Acta Crystallogr., B35 (1979) 2020.
23 A. Almennigen, E. Gard, A. Haaland and J. Brunvoll, J. Organomet. Chem., 107 (1976) 273.
24 L. Hedberg and K.J. Hedberg, Chem. Phys., 53 (1970) 1228; P. Seiler and J.D. Dunitz, Acta Crystallogr., B36 (1980) 2255.
25 D.P. Freyberg, J.L. Robbins, K.N. Raymond and J.C. Smart, J. Am. Chem. Soc., 101 (1979) 892.
26 Yu.T. Struchkov, V.G. Andrianov, T.N. Sal'nikova, I.R. Lyatifov and R.B. Materikova, J. Organomet. Chem., 145 (1978) 213.
27 X-Ray: N.C. Webb and R.E. Marsh, Acta Crystallogr., 22 (1967) 382; ^{13}C NMR: G. Stringer, D. Phil. Thesis, Oxford University, 1988.
28 P.M. Treichel, J.W. Johnson and J.C. Calabrese, J. Organomet. Chem., 88 (1975) 215.

29 E.O. Fischer, D. Seus and R. Jira, Z. Naturforsch., 813 (1953) 692; P.L Paulson and G. Wilkinson, J. Am. Chem. Soc., 76 (1954) 2024.
30 H.B. Fritz, F.H. Köhler and K.E. Schwarzhans, J. Organomet. Chem., 16 (1969) 14.
31 H.B. Fritz, F.H. Köhler and K.E. Schwarzhans, J. Organomet. Chem., 19 (1969) 449.
32 T.K. Miyamoto, M. Tsutsui and L.-B. Chen, Chem. Lett., (1981) 729.
33 S.J. Pugh, J.C. Green, S.A. Westcott, A.K. Kakkar, G. Stringer and T.B. Marder, unpublished results.
34 J. Trotter, Acta Crystallogr., 11 (1958) 355.
35 N.G. Parsonage, and L.A.K. Staveley, Disorder In Crystals, Clarendon Press, Oxford, 1978, pp. 640–655.
36 N.S. Crossley, J.C. Green, A. Nagy and G. Stringer, J. Chem. Soc., Dalton Trans., (1989) 2139.
37 See [13] and references therein.
38 R.M. Kowaleski, A.L. Rheingold, W.C. Trogler and F. Basolo, J. Am. Chem. Soc., 108 (1986) 2460.
39 A.E. Smith, Inorg. Chem., 11 (1972) 165.